

## Multicolour spectral karyotyping of mouse chromosomes

Marek Liyanage<sup>1</sup>, Allen Coleman<sup>2</sup>, Stan du Manoir<sup>1</sup>, Tim Veldman<sup>1</sup>, Stephen McCormack<sup>3</sup>, Robert B. Dickson<sup>3</sup>, Carolee Barlow<sup>4</sup>, Anthony Wynshaw-Boris<sup>4</sup>, Siegfried Janz<sup>2</sup>, Johannes Wienberg<sup>5</sup>, Malcolm A. Ferguson-Smith<sup>5</sup>, Evelin Schröck<sup>1</sup> & Thomas Ried<sup>1</sup>

Murine models of human carcinogenesis are exceedingly valuable tools to understand genetic mechanisms of neoplastic growth. The identification of recurrent chromosomal rearrangements by cytogenetic techniques serves as an initial screening test for tumour specific aberrations. In murine models of human carcinogenesis, however, karyotype analysis is technically demanding because mouse chromosomes are acrocentric and of similar size. Fluorescence *in situ* hybridization (FISH) with mouse chromosome specific painting probes<sup>1</sup> can complement conventional banding analysis. Although sensitive and specific, FISH analyses are restricted to the visualization of only a few mouse chromosomes at a time. Here we apply a novel imaging technique<sup>2</sup> that we developed recently for the visualization of human chromosomes<sup>3</sup> to the simultaneous discernment of all mouse chromosomes. The approach is based on spectral imaging to measure chromosome-specific spectra after FISH with differentially labelled mouse chromosome painting probes. Utilizing a combination of Fourier spectroscopy, CCD-imaging and conventional optical microscopy, spectral imaging allows simultaneous measurement of the fluorescence emission spectrum at all sample points. A spectrum-based classification algorithm has been adapted to karyotype mouse chromosomes. We have applied spectral karyotyping (SKY) to chemically induced plasmocytomas, mammary gland tumours from transgenic mice overexpressing the *c-myc* oncogene and thymomas from mice deficient for the ataxia telangiectasia (*Atm*) gene. Results from these analyses demonstrate the potential of SKY to identify complex chromosomal aberrations in mouse models of human carcinogenesis.

We performed spectral karyotyping (SKY) on a normal mouse metaphase spread prepared from splenocytes of the FVB mouse (Fig. 1). The chromosome specific painting probes were generated by high resolution flow sorting<sup>1</sup> and were labelled either singly with Spectrum Green, Cy3, Texas Red, Cy5, or Cy5.5 or in combinations (Table 1). The differentially labelled probe pools were combined and hybridized together with an excess of unlabelled Cot-1 fraction of mouse genomic DNA to mouse metaphase chromosome preparations. Chromosome-specific spectra were measured using spectral imaging. Spectral imaging combines Fourier spectroscopy, CCD-imaging and optical microscopy to measure the fluorescence emission spectrum simultaneously

**Table 1** Fluorescence labelling scheme of mouse chromosomes

Chromosome	Spec. green	Cy5	Cy3	Texas red	Cy5.5
1	+	+	+		
2		+			+
3			+		+
4	+		+	+	
5		+	+		
6	+		+		+
7	+			+	
8			+	+	
9					+
10		+			
11		+		+	
12	+	+			+
13		+	+	+	
14		+	+		+
15	+		+		
16			+		
17				+	+
18	+	+		+	
19	+				+
X	+				
Y				+	

at all image points (pixels) after a single exposure<sup>2,3</sup>. Therefore, spectral imaging is significantly different from conventional fluorescence imaging techniques for FISH experiments based on fluorochrome-specific optical filters and multiple subsequent exposures<sup>4</sup>. The spectral measurement of the hybridization was visualized by assigning a red, green and blue (RGB) look-up table to specific sections of the emission spectrum (Fig. 1*b*, see Methods). For instance, the X-chromosome, labelled only with Spectrum Green appears blue, chromosome 16 (Cy3) appears green, and chromosome 2 (Cy5 and Cy5.5) appears red (Fig. 1*b*). The RGB display allows the assessment of important parameters of the hybridization, e.g., intensity and homogeneity (Fig. 1*b*). Based on the measurement of discrete emission spectra at all pixels of the image, the hybridization colours are then converted by applying a spectral classification algorithm that results in the assignment of a discrete colour to all pixels with identical spectra (Fig. 1*c*). The spectral classification is the basis for chromosome identification (Fig. 1*c*) and spectral karyotyping (Fig. 1*d*).

Murine models of human carcinogenesis are widely used to delineate genetic mechanisms that determine tumour initiation and progression<sup>5</sup>. The study of chromosomal aberrations in mouse models, however, is extremely demanding because mouse chromosomes are difficult to discern and subtle aberrations often remain unrecognized. The potential of spectral karyotyping as a genome scanning method for detection of chromosomal aberrations in mouse metaphase spreads was explored by analysing metaphase chromosomes from different mouse models of human carcinogenesis: (i) in chemically induced plasmocytomas in BALB/c mice, (ii) in mammary gland tumours that developed in transgenic animals that overexpress the *c-myc* gene under the control of the MMTV-promotor and (iii) in thymomas that occurred in mice deficient for the ataxia telangiectasia (*Atm*) gene.

Mice from susceptible strains (BALB/c) treated with pristane oil develop, in a multistep process, tumours that are histomorphologically and immunologically similar to human plasmocytomas<sup>6</sup>. The cytogenetic hallmark of

<sup>1</sup>Diagnostic Development Branch and  
<sup>4</sup>Laboratory of Genetic Disease Research, National Center for Human Genome Research, National Institutes of Health, Bldg. 49, 49 Convent Drive, Rm. 4A28, Bethesda, Maryland 20892-4470, USA

<sup>2</sup>Laboratory of Genetics, National Cancer Institute, National Institutes of Health, Bethesda, Maryland, USA  
<sup>3</sup>Lombardi Cancer Center, Georgetown University, Washington, D.C., USA

<sup>5</sup>Department of Pathology, Cambridge University, Cambridge, UK

Correspondence should be addressed to T.R.  
e-mail: tried@nchgr.nih.gov

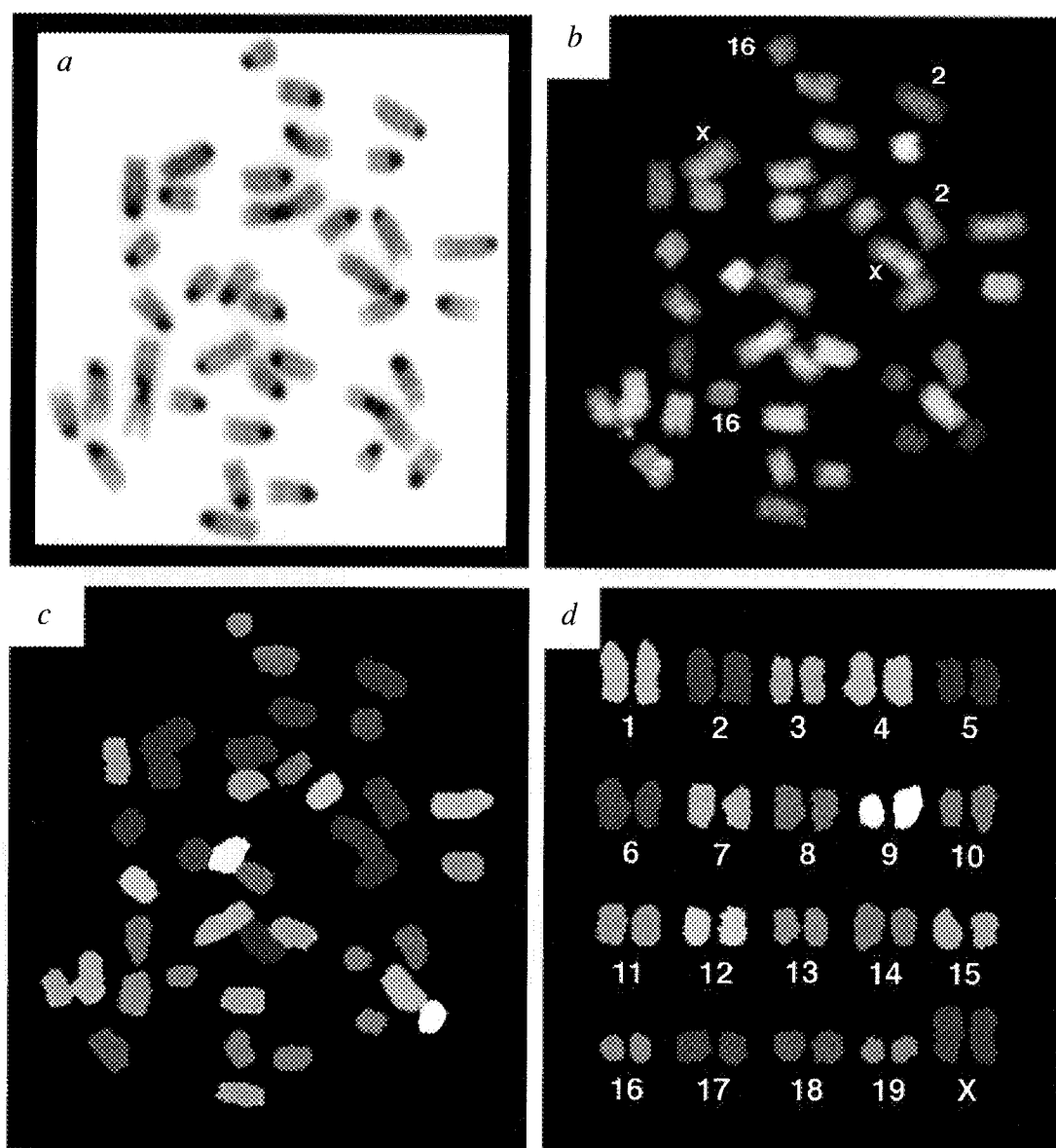


Fig. 1 Spectral karyotyping (SKY) of mouse chromosomes. *a*, Metaphase spread from normal mouse splenocytes (Strain: FVB). The inverted image of the DAPI-stained chromosomes results in a G-like banding pattern. *b*, Same metaphase as in (*a*) after simultaneous hybridization of 21 differentially labelled mouse chromosome painting probes. The display colours allow discernment of most chromosomes in different colours. However, chromosome painting probes that were labelled with similar fluorochromes appear in similar colours. The numbers denote chromosomes that were labelled with green (X-chromosome), red (chromosome 16) or near infrared (chromosome 2) fluorochromes only. *c*, Spectral classification of the same metaphase spread shown in (*a*, *b*). Based on pixel by pixel measurement of the spectra of the entire image, the display colours in (*b*) were converted to classification colours. Here, all pixels that have identical spectra were assigned the same classification colour. *d*, The spectral classification forms the basis for colour karyotyping of mouse chromosomes. All mouse chromosomes can be discerned according to a specific colour.

pristine-induced plasmocytoma in mice is the chromosomal translocation  $t(12;15)$  that juxtaposes the *c-myc* oncogene in the vicinity of promoters for the immunoglobulin heavy chain genes on mouse chromosome 12 (ref. 6). The genetic consequence of the mouse translocation  $t(12;15)$  is therefore similar to the translocation  $t(8;14)$  observed in human Burkitt's lymphoma. However, it is not clear whether tumour progression depends on additional chromosomal aberrations and conventional cytogenetic analysis has not detected further recurrent chromosomal aberrations. We examined the entire chromosome complement from a mouse plasmocytoma (X24) by SKY on metaphase chromosomes. In this hypotetraploid tumour, the translocation

$t(12;15)$ , identified by G-banding, was readily confirmed. In addition, unrecognized rearrangements were detected. In all cells analysed ( $n = 9$ ) a reciprocal translocation  $t(3;6)$  and a translocation  $t(1;X)$  were identified (Fig. 2*a*). The analysis of a larger number of tumours using SKY will reveal if similar aberrations occur consistently in mouse plasmocytomas, and the fine mapping of the translocation breakpoints will guide the search for candidate genes.

The analysis of a sequence of chromosomal aberrations that occur during the development of human breast carcinomas is arduous. This is in strong contrast to, for example, colon carcinogenesis<sup>7</sup> and is mainly attributable to the difficulty of retrieving tumour mate-

rial at defined stages of human breast carcinogenesis. It is clear, however, that a recurrent pattern of chromosomal aberrations occurs in breast carcinomas and that the gain of function of certain oncogenes, such as the *c-myc* oncogene, is a crucial genetic aberration<sup>8</sup>. Transgenic mice that overexpress oncogenes hold great promise in unravelling genomic effects of oncogene gain-of-function mutations because they will allow the study of chromosomal aberrations that occur during tumour initiation and progression<sup>9</sup>. Transgenic mice that express the *c-myc* oncogene under MMTV-promotor control develop mammary gland tumours at the age of 9 to 12 months<sup>10</sup>. We analysed metaphase spreads from one of these tumours<sup>11</sup> by SKY in order to identify and map chromosomal aberrations (Fig. 2b). Numerous rearrangements were identified that occurred in the majority (90%) of the cells ( $n = 11$ ): a loss of the X chromosome, trisomy for chromosome 18, a translocation  $t(X;11)$  and a dicentric marker chromosome that is derived from chromosome 4. The identification of this dicentric marker chromosome is particularly interesting because it indicates that the formation of a dicentric marker does not preclude proper chromosome segregation during mitotic cell division. Compared to G-banding alone, SKY will allow large numbers of tumours to be analysed reliably and rapidly. This may provide insight into *c-myc* induced chromosomal changes in murine mammary gland tumorigenesis.

The biological and genetic significance of tumour suppressor gene function can be elegantly studied in mice<sup>12</sup>. For example, we have studied tumours that developed in mice that have homozygous disruption of the *Atm* gene<sup>13</sup>. Humans afflicted with ataxia telangiectasia (AT) have, among a plethora of other symptoms, an increased risk for the development of malignant tumours, most commonly lymphomas. *Atm*-deficient mice have virtually all of the findings of AT patients. Of note, thymic lymphomas were observed invariably between 2 and 4 months of age<sup>13</sup>. We analysed the chromosomal consequences of *Atm* inactivation in one of the thymomas using SKY (Fig. 2c). We examined 12 metaphases; increased genomic instability was reflected by a marked heterogeneity of chromosomal aberrations in metaphase spreads of this tumour. We detected an involvement of chromosomes 14 in all metaphase spreads, suggesting an important role of genes on this chromosome in

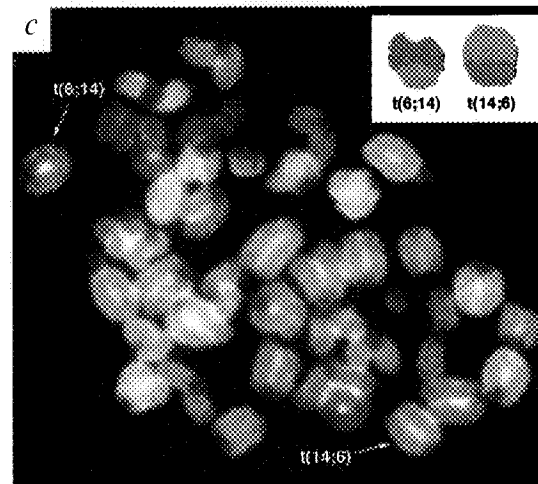
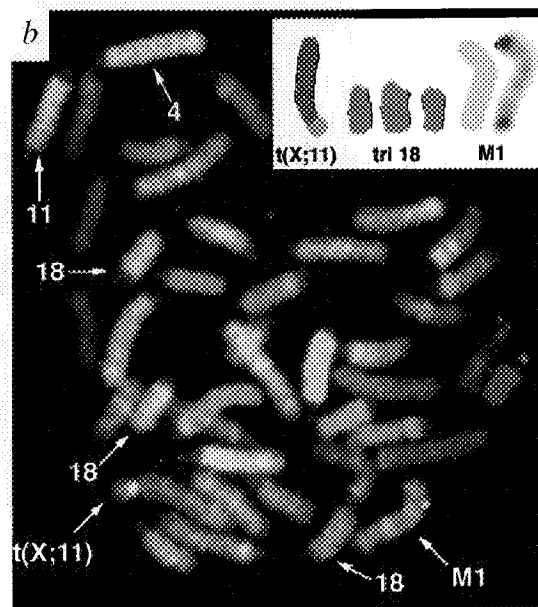
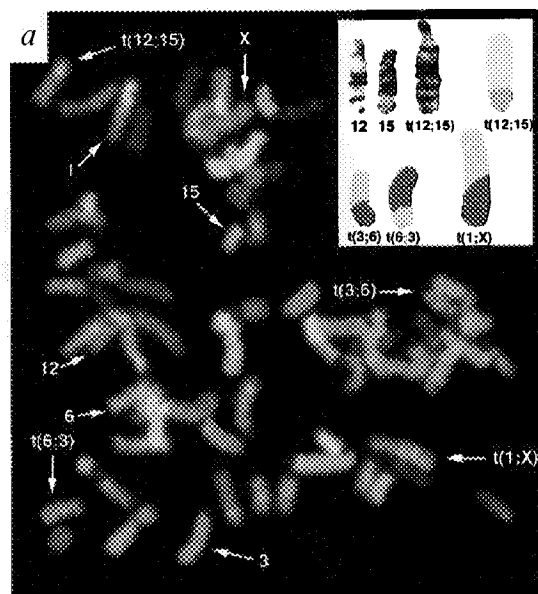


Fig. 2 Applications of SKY to identify chromosomal aberrations in murine models of carcinogenesis. a, Metaphase spread from a mouse plasmocytoma (XRPC24). Several chromosomal translocations were detected. SKY confirmed the presence of a translocation  $t(12;15)$  which had already been identified by G-banding analysis (inset). Previously unrecognized chromosomal aberrations not detected by chromosome banding alone include a reciprocal translocation involving chromosomes 3 and 6 as well as a translocation  $t(1;X)$ . Arrows denote the aberrant chromosomes in metaphase and their normal homologues. The spectra based classification of all aberrant chromosomes is presented (inset). b, Metaphase spread from a cell line established from a mammary gland carcinoma that developed in *c-myc* transgenic mice. Several previously unknown aberrations were identified: translocation  $t(X;11)$ , trisomy 18, and a marker chromosome (M1) derived from chromosome 4. Arrows denote the aberrant chromosomes in metaphase and their normal homologues. The spectrum-based classification and the DAPI-banding of the marker M1 is shown (inset). c, Identification of chromosomal aberrations in metaphase cells of primary cultures from a thymoma that developed in mice with homozygous inactivation of the ataxia telangiectasia (*Atm*) gene. The reciprocal translocation  $t(6;14)$  was readily identified (arrows). The aberration was confirmed by spectra-based classification (inset).

tumorigenesis (Fig. 2c). Chromosome 14 carries the genes for T-cell receptor chains  $\alpha$  and  $\delta$ . Similar involvement of T-cell receptor genes was observed in lymphomas diagnosed in AT-patients<sup>14</sup>. This suggests common genetic mechanisms in human AT and murine *Atm*-deficiency. Based on the SKY-results, a targeted analysis of candidate genes will allow the further elucidation of genetic pathways involved in the genesis of malignant thymomas.

We have shown that spectral karyotyping is a reliable and robust screening test that is broadly applicable to the detection of chromosomal aberrations in murine models of tumorigenesis. SKY will assist in the identification of regions that are recurrently altered in mouse model systems by delineating consistent chromosomal breakpoints. Other applications of SKY will extend to the interspecies analysis of chromosomal aberrations in related animal models, such as hamster or rat, and will become an important tool to automate the analysis of a large number of metaphase spreads for mutagenicity testing in experimental toxicology.

### Methods

**Preparation of mouse metaphase chromosomes.** Mouse metaphase chromosomes were prepared from LPS-stimulated spleen cultures, from cell lines established from transgenic mice, or from short term cultures according to standard procedures, and fixed in methanol acetic acid. The suspensions were dropped onto precleaned slides and rinsed with acetic acid to remove excess cytoplasm. The preparations were dehydrated through an ethanol series and stored at room temperature.

**Amplification and labelling of flow sorted mouse chromosomes.** Mouse chromosomes were isolated by high resolution flow sorting as described<sup>1</sup>. Chromosomes were amplified using degenerate oligonucleotide primed PCR (DOP-PCR)<sup>15</sup>. The individual probe pools were labelled using DOP-PCR by direct incorporation of haptenized or fluorochrome conjugated nucleotides in the combination described in Table 1.

**In situ hybridization and detection.** Approximately 100 ng of the labelled probe pools for each mouse chromosome were precipitated in the presence of 30  $\mu$ g of the Cot-1 fraction of mouse genomic DNA (Bethesda Research Laboratories). The probe cocktail was resuspended in 50% formamide, 10% dextran sulfate, 2 $\times$  SSC and denatured (5 min, 80 °C) followed by a pre-

annealing step for 1 h at 37 °C. After hybridization at 37 °C for 2 days, the slides were washed, and the haptenized probe sequences detected: biotin labelled sequences were detected using avidin Cy5, and the digoxigenin labelled sequences were detected using a mouse anti-digoxigenin antibody followed by a goat anti-mouse antibody conjugated to Cy5.5 (Amersham Life Sciences). Samples were counterstained with DAPI and embedded in an antifade reagent (para-Phenylenediamine).

**Spectral imaging.** The spectral analysis is based on the spectral cube system (SD200, Applied Spectral Imaging). Imaging and analysis were performed as described<sup>2,3</sup>. The SD200 imaging system was attached to an inverted microscope (Leica DMIRBE) via a C-mount. It consists of an optical head with a special Fourier transform spectrometer (Sagnac common path interferometer) to measure the spectrum and a cooled CCD camera (Princeton Instruments) for imaging. The samples were illuminated with a Xenon lamp (OptiQuip 770/1600) and imaged with a 63x oil immersion objective through a custom designed filter set (Chroma Technology) with broad emission bands (excitation filter: 486/28, 565/16, 642/22; emission filter: 524/44, 600/38, 720/113; beamsplitter: reflection 421–480, 561–572, 631–651, transmission 495–564, 580–620, 660–740). The use of this filter allows the simultaneous excitement of all dyes and the measurement of their emission spectra. Therefore, a single exposure (approximately 1 min depending on the brightness of the preparation) is sufficient to acquire the entire image. The conversion of emission spectra to visualize the spectral image in display colours is achieved by assigning a different colour (blue, green, red) to specific spectral ranges. The intensity for each colour is proportional to the integrated intensity in the corresponding spectral range (Fig. 1b). The spectral classification that is independent of signal intensities enables multiple different spectra in the image to be identified and highlighted in classification-colours (Fig. 1c). This allows assignment of a specific classification-colour to all mouse chromosomes based on their spectra alone (Fig. 1d). The algorithm is described in detail<sup>3</sup>.

### Acknowledgements

We thank M. Potter, D. Soenksen and Y. Garini for valuable discussions. E.S. received a fellowship from the Deutsche Forschungsgemeinschaft. R.B.D. was supported by grant # DAMD-17-94-J-4257 and S.M. by grant # NIH-1P50CA58185.

Received 23 July; accepted 9 September 1996.

- Rabbits, P. et al. Chromosome specific paints from a high resolution flow karyotype of the mouse. *Nature Genet.* **9**, 369–375 (1995).
- Malik, Z. et al. Fourier transform multipixel spectroscopy for quantitative cytology. *J. Microscopy* **182**, 133–140 (1996).
- Schröck, E. et al. Multicolor spectral karyotyping of human chromosomes. *Science* **273**, 494–497 (1996).
- Speicher, M.R., Ballard, S.G. & Ward, D.C. Karyotyping human chromosome by combinatorial multi-fluor FISH. *Nature Genet.* **12**, 368–375 (1996).
- Kastan, M. Experimental models of human carcinogenesis. *Nature Genet.* **5**, 207–208 (1993).
- Potter, M. & Wiener, F. Plasmocytomagenesis in mice: model of neoplastic development dependent upon chromosomal translocations. *Carcinogenesis* **13**, 1681–1697 (1992).
- Fearon, E.R. & Vogelstein, B. A genetic model for colorectal carcinogenesis. *Cell* **61**, 759–767 (1990).
- Bieche, I. & Lidereau, R. Genetic alterations in breast cancer. *Genes Chrom. Cancer* **4**, 227–251 (1995).
- Cardiff, R.D. & Muller, W.J. Transgenic models of mammary tumorigenesis. *Cancer Surveys* **16**, 97–113 (1993).
- Leder, A., Pattengale, P.K., Kuo, A., Stewart, T. & Leder, P. Consequences of widespread deregulation of the *c-myc* gene in transgenic mice: multiple neoplasms and normal development. *Cell* **45**, 485–495 (1986).
- Amundadottir, L.T. et al. TGF $\alpha$  and *c-myc* cooperation in mouse mammary tumorigenesis: coordinate stimulation of growth and suppression of apoptosis. *Oncogene* **13**, 757–765 (1996).
- Capecchi, M.R. Altering the genome by homologous recombination. *Science* **244**, 1288–1292 (1989).
- Barlow, C. et al. *Atm*-deficient mice: a paradigm of ataxia telangiectasia. *Cell* **86**, 159–171 (1996).
- Taylor, A.M., Metcalfe, J.A., Thick, J. & Mak, Y.F. Leukemia and lymphoma in ataxia telangiectasia. *Blood* **87**, 423–438 (1996).
- Telenius, H. et al. Cytogenetic analysis by chromosome painting using DOP-PCR amplified flow sorted chromosomes. *Genes Chrom. Cancer* **4**, 267–263 (1992).